Article
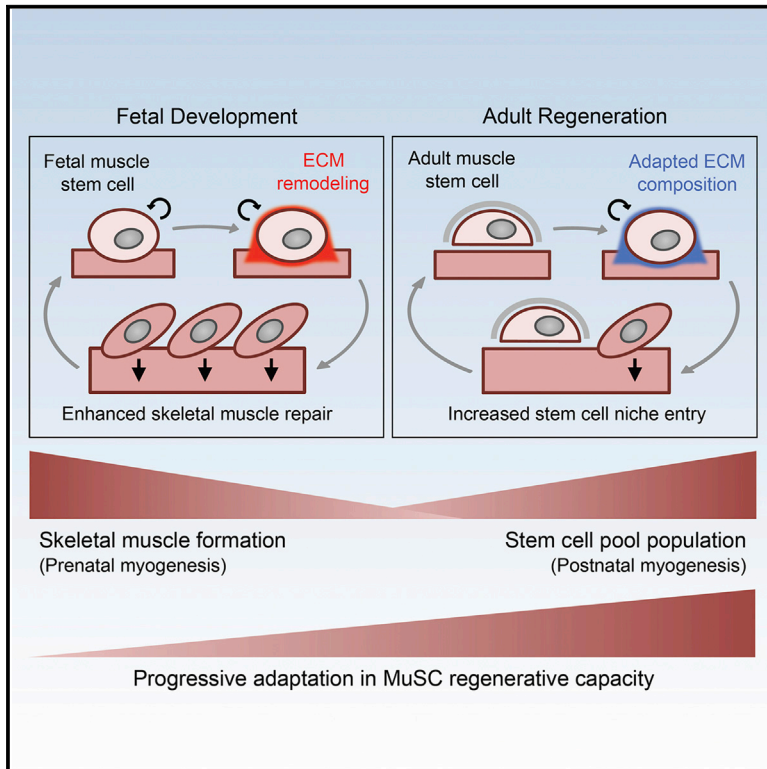
Autonomous Extracellular Matrix Remodeling Controls a Progressive Adaptation in Muscle Stem Cell Regenerative Capacity during Development

Graphical Abstract

Authors

Matthew Timothy Tierney,
Anastasia Gromova,
Francesca Boscolo Sesillo, David Sala,
Caroline Spenlé, Gertraud Orend,
Alessandra Sacco

Correspondence

asacco@sbpdiscovery.org

In Brief

Tierney et al. demonstrate that fetal muscle stem cells exhibit a distinct regenerative capacity, preferentially contributing to skeletal muscle growth before their potential for stem cell pool repopulation increases during adulthood. This is controlled by autonomously remodeling their microenvironment with the production of tenascin-C, fibronectin, and collagen VI.

Highlights

- Fetal MuSCs resist progenitor specification and efficiently expand upon transplant

- Balance between MuSC-mediated muscle repair and niche entry shifts postnatally

- Fetal MuSCs remodel their microenvironment via ECM protein deposition

- Tenascin-C, fibronectin, and collagen VI play stage-specific roles in MuSC function

Accession Numbers

GSE76989

CellPress

OPEN
ACCESS
CellPress

Cell Reports
Article

Autonomous Extracellular Matrix Remodeling Controls a Progressive Adaptation in Muscle Stem Cell Regenerative Capacity during Development

Matthew Timothy Tierney,[1,2] Anastasia Gromova,[2,3] Francesca Boscolo Sesillo,[1,2] David Sala,[2] Caroline Spenlé,[4,5,6,7] Gertraud Orend,[4,5,6,7] and Alessandra Sacco[2,*]

[1]Graduate School of Biomedical Sciences, Sanford Burnham Prebys Medical Discovery Institute, 10901 N. Torrey Pines Road, La Jolla, CA 92037, USA
[2]Development, Aging and Regeneration Program, Sanford Burnham Prebys Medical Discovery Institute, 10901 N. Torrey Pines Road, La Jolla, CA 92037, USA
[3]Biomedical Sciences Graduate Program, University of California, San Diego, 9500 Gilman Drive, La Jolla, CA 92093-0685, USA
[4]Inserm U1109, MN3T Team, The Microenvironmental Niche in Tumorigenesis and Targeted Therapy, 3 Avenue Molière, 67200 Strasbourg, France
[5]Université de Strasbourg, 67000 Strasbourg, France
[6]LabEx Medalis, Université de Strasbourg, 67000 Strasbourg, France
[7]Fédération de Médecine Translationnelle de Strasbourg (FMTS), 67000 Strasbourg, France
*Correspondence: asacco@sbpdiscovery.org
http://dx.doi.org/10.1016/j.celrep.2016.01.072

SUMMARY

Muscle stem cells (MuSCs) exhibit distinct behavior during successive phases of developmental myogenesis. However, how their transition to adulthood is regulated is poorly understood. Here, we show that fetal MuSCs resist progenitor specification and exhibit altered division dynamics, intrinsic features that are progressively lost postnatally. After transplantation, fetal MuSCs expand more efficiently and contribute to muscle repair. Conversely, niche colonization efficiency increases in adulthood, indicating a balance between muscle growth and stem cell pool repopulation. Gene expression profiling identified several extracellular matrix (ECM) molecules preferentially expressed in fetal MuSCs, including tenascin-C, fibronectin, and collagen VI. Loss-of-function experiments confirmed their essential and stage-specific role in regulating MuSC function. Finally, fetal-derived paracrine factors were able to enhance adult MuSC regenerative potential. Together, these findings demonstrate that MuSCs change the way in which they remodel their microenvironment to direct stem cell behavior and support the unique demands of muscle development or repair.

INTRODUCTION

Muscle stem cells (MuSCs), also termed satellite cells, reside in a quiescent state in adult tissues, poised to respond in the event of injury and directly mediate skeletal muscle regeneration (Lepper et al., 2011; Sambasivan et al., 2011). Once activated, MuSCs can self-renew while generating myogenic progenitors to repair damaged tissue (Rocheteau et al., 2012; Sacco et al., 2008; Zammit et al., 2004). During the regenerative process, MuSCs also repopulate the stem cell pool by colonizing the satellite cell niche, under the basal lamina and adjacent to the myofiber (Collins et al., 2005; Montarras et al., 2005; Shea et al., 2010). Thus, the balance between the continued generation of differentiated progeny and re-entry into quiescence largely determines the efficacy and long-term sustainability of skeletal muscle growth and repair.

Adult MuSC precursors originate during developmental myogenesis and are primarily responsible for muscle formation and growth, ultimately populating the adult stem cell pool (Gros et al., 2005; Kassar-Duchossoy et al., 2005; Relaix et al., 2005). While a well-coordinated extrinsic regulatory system influences MuSC fate during development (Bentzinger et al., 2012), MuSCs also exhibit different behavioral characteristics and responsiveness to external stimuli during prenatal development (Biressi et al., 2007; Hutcheson et al., 2009). Recent work has identified genes able to promote the transition from embryonic to fetal myogenesis, including Nfix and Pitx2/3 (L'honoré et al., 2014; Messina et al., 2010). Still, the factors controlling functional progression of MuSCs throughout development and into adulthood are poorly understood.

The MuSC microenvironment dynamically changes in developing muscle as they begin to occupy and physically interact with the newly formed satellite cell niche during late fetal stages (Kassar-Duchossoy et al., 2005; Relaix et al., 2006). Extracellular matrix (ECM) proteins are critical components of stem cell niches and are able to direct stem cell fate. Both fibronectin and collagen VI have been recently shown to impact adult MuSC self-renewal through increased non-canonical Wnt signaling or altered biomechanical properties (Bentzinger et al., 2013; Urciuolo et al., 2013). Additionally, MuSCs themselves can control cell adhesion and basal lamina formation in the emerging satellite cell niche (Bröhl et al., 2012). However, much is still unknown about how these

ECM proteins reciprocally interact with MuSC to control their functional properties during muscle development.

To investigate the role played by MuSCs in directing their functional progression during muscle development, we performed comparative analyses on MuSCs isolated throughout myogenesis. We demonstrate that fetal MuSCs are uniquely able to resist advancement to the progenitor stage and can expand more efficiently than their adult counterparts following transplantation. These properties coincide with the enhanced ability to remodel their local microenvironment with several ECM proteins, including tenascin-C, fibronectin, and collagen VI. Co-transplantation and loss-of-function experiments reveal that these ECM components are critical and stage-specific regulators of MuSC function. Overall, our findings indicate that fetal MuSCs provide instructive cues and govern cell fate decisions through the autonomous deposition of ECM molecules, favoring their direct contribution to skeletal muscle repair.

RESULTS

Fetal MuSCs Resist Myogenic Lineage Progression

We investigated the potential behavioral differences between MuSCs taken at various developmental stages by purifying cells via fluorescence-activated cell sorting (FACS) based on α7-integrin and CD34 expression, previously shown to efficiently isolate adult MuSCs (Sacco et al., 2008). α7-integrin expression defined the myogenic fraction in fetal muscle cells (Figures S1A and S1B). CD34 expression was associated with a higher percentage of cells expressing Pax7, a paired box transcription factor marking MuSCs (Seale et al., 2000), and a lower percentage of cells expressing Myod1, a bHLH transcription factor defining progression to the progenitor stage (Davis et al., 1987; Figure S1B). Cells expressing both α7-integrin and CD34 in fetal, neonatal (postnatal day 7), and juvenile (postnatal day 21) samples were enriched for a population expressing Pax7 (Figures 1A and S1C). MuSCs from all four developmental stages demonstrated comparable myogenicity when cultured in differentiation conditions; however, fetal MuSCs were less fusogenic than their postnatal counterparts, suggesting that fusion efficiency increases during development (Figures S1D and S1E). This is consistent with previous findings (Biressi et al., 2007).

As adult MuSCs progress to the progenitor stage following their activation in culture (Brack et al., 2008; Gilbert et al., 2010; Montarras et al., 2005), we asked whether this behavior was conserved throughout development. Notably, fetal MuSCs resisted Myod1 upregulation when cultured in growth conditions, unlike the uniform upregulation of Myod1 in postnatal MuSCs (Figures 1B and S1F). qRT-PCR analysis revealed that fetal MuSCs expressed lower levels of *Myod1* upon isolation and *Myf5*, *Myod1*, and *Myog* when cultured while maintaining comparable levels of *Pax7* expression (Figure 1C). At the protein level, fetal MuSCs that did not upregulate Myod1 maintained Pax7 expression while actively dividing, as indicated by EdU incorporation (Figures 1D and S1G). This was consistent in situ when associated with freshly isolated single myofibers as Pax7$^+$Myod1$^-$ MuSCs were found during late fetal development (embryonic day 18.5 [E18.5]), but not at early postnatal time points (postnatal da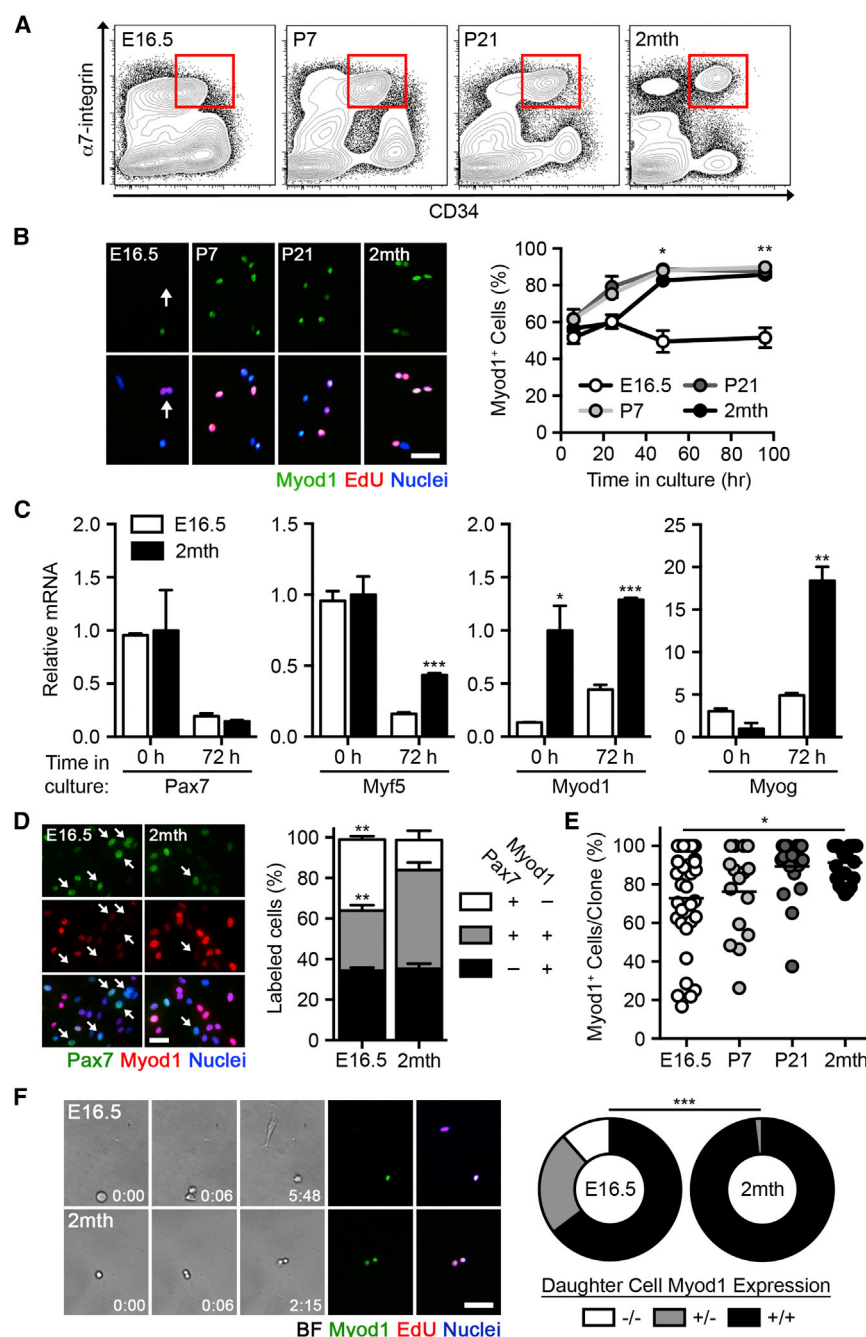y 10 [P10]; Figure S1H). In differentiation conditions, fetal MuSCs expressed higher levels of *Pax7* and lower levels of both *Myf5* and *Myog* (Figure S1I).

We next asked whether all or only a subset of fetal MuSCs were capable of delaying Myod1 upregulation. Clonal analyses revealed heterogeneity in fetal MuSCs as 18.2% of clones maintained more than half of their progeny as Myod1$^-$ cells (Figure 1E). This ability was progressively lost during postnatal development, as Myod1 was expressed in the majority of the progeny in all adult MuSC clones. Clone size and the frequency of clone formation were not significantly different among the MuSC populations analyzed (Figure S1J). Clone size also did not correlate with the percentage of Myod1$^+$ cells within each clone, indicating that myogenic lineage progression was not influenced by the rate of cell proliferation (Figure S1K).

Population heterogeneity can be achieved via different rates of asymmetric or symmetric divisions (Dumont et al., 2015). To assess the ability of fetal MuSCs to utilize these modes of division while proliferating in culture, we monitored MuSCs by time-lapse microscopy and retrospectively immunostained for Myod1 expression. Fetal MuSCs more frequently underwent symmetric expansion and asymmetric division events than adult MuSCs and exhibited a reduced frequency of symmetric depletion events, indicating that they possess intrinsic differences in cell division dynamics (Figure 1F; Movies S1 and S2). It should be noted that our retrospective assessment of Myod1 expression is not able to distinguish between daughter cell fate acquisition during or after cell division has occurred. All together, these data indicate that cultured fetal MuSCs are delayed in their progression through the myogenic program.

Fetal MuSCs Exhibit Enhanced Regenerative Potential

We reasoned that the differential behavior of fetal MuSCs might allow them to more effectively maintain self-renewal potential in a regenerative setting. To test this, transplantation experiments were performed (Sacco et al., 2008, 2010). We injected MuSCs from transgenic mice expressing EGFP and firefly luciferase into the tibialis anterior (TA) muscle of non-obese diabetic/severely combined immunodeficient (*NOD/SCID*) mice, locally irradiated to deplete endogenous MuSCs and favor donor cell engraftment (Heslop et al., 2000; Figure 2A). Consistent with our results in vitro, a smaller portion of GFP$^+$ donor fetal MuSCs expressed Myod1 compared to adult MuSCs 3 days after transplantation (Figure 2B). In addition, a higher proportion of fetal MuSCs maintained Pax7 expression at this early time point, resulting in a larger total pool of Pax7$^+$ cells (Figures 2B and S2A). Proliferation dynamics were evaluated by non-invasive bioluminescence imaging (BLI) (Sacco et al., 2008). Strikingly, fetal MuSCs were capable of increased expansion during the initial phases of regeneration, ultimately engrafting at levels ∼8-fold higher than adult MuSCs when transplanting 1,000 cells (Figures 2C, 2D, and S2B). Limiting dilution assays demonstrated an increased rate of successful fetal MuSC engraftments following the delivery of only ten cells (Figures 2D and S2B). The average amount of light emitted per nucleus in fetal and adult MuSCs was not significantly different, confirming that the increase in BLI was due to an increase in donor cell number (Figure S2C). No differences in cell number were observed 1 day post-transplantation, and fetal MuSCs did not exceed adult

Figure 1. Fetal MuSCs Resist Progression to the Progenitor Stage

(A) Fluorescent-based cell sorting (FACS) of MuSCs from hind limb muscles.

(B) Images of freshly isolated MuSCs cultured in growth conditions and pulsed with EdU for 4 hr. The scale bar represents 50 μm (left). Quantification of the percentage of Myod1^{+} cells is shown (n = 3–6; right).

(C) *Pax7*, *Myf5*, *Myod1*, and *Myog* mRNA levels in MuSCs, freshly isolated or cultured in growth conditions (n = 3–5).

(D) Images of freshly isolated MuSCs cultured for 4 days in growth conditions. The scale bar represents 10 μm (left). Quantification of the percentage of Pax7[±] Myod1[±] cells is shown (n = 3; right).

(E) Quantification of the percentage of Myod1^{+} cells within individual clones cultured in growth conditions (n = 15–33 clones).

(F) Frames from a MuSC time-lapse recording (min:s) and retrospective immunofluorescence of Myod1[±] EdU[±] cells. The scale bar represents 10 μm (left). Quantification of symmetric expansion (−/−), asymmetric division (+/−), or symmetric depletion (+/+) divisions is shown (n = 101–135 divisions; right).
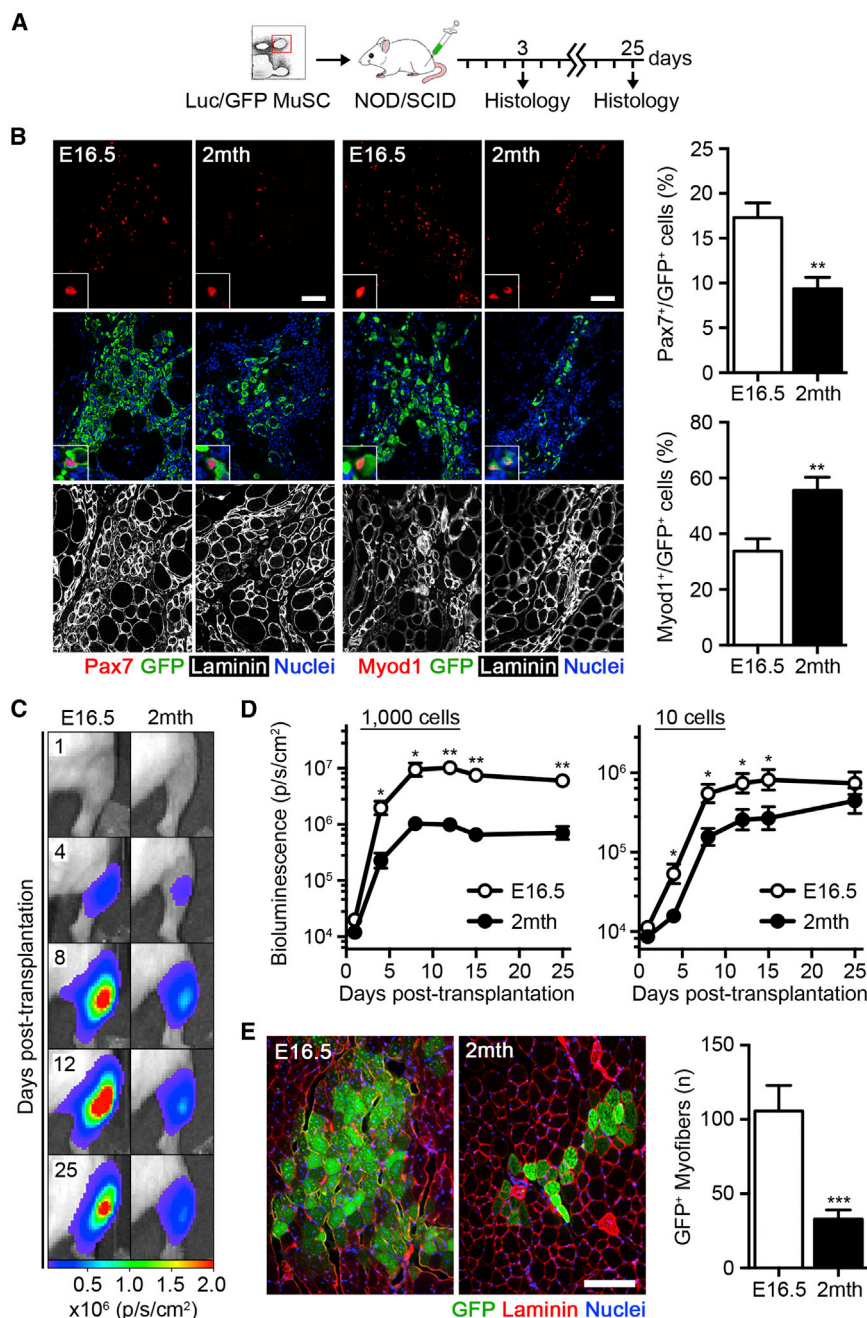
Data are represented as average ± SEM (***p < 0.001, **p < 0.01, and *p < 0.05). See also Figure S1 and Movies S1 and S2.

To complement the use of cell surface markers to isolate MuSCs, we utilized the *Pax7-CreER^TM* driver (Nishijo et al., 2009) crossed with the *R26R^TdT* allele (Madisen et al., 2010). Tamoxifen (tmx) was administered to time-mated females or adult mice to activate the TdTomato reporter gene in Pax7-expressing cells, enabling the isolation of fetal and adult MuSCs (Figure S3A). Additionally, Pax7^{+} MuSCs were isolated from regenerating adult muscle 3 days post-barium chloride (BaCl$_2$) injury (Figures S3C and S3D) to investigate the potential effect of activation on MuSC regenerative potential. Histological and FACS analyses validated the efficient labeling of MuSCs at both fetal and adult stages (Figures S3B–S3D). Whereas virtually all labeled cells were found to express α7-integrin,

MuSCs until after 3 days, suggesting no apparent difference in cell survival (Figure S2D). Indeed, no differences in the percentage of apoptotic, TUNEL+ donor cells were observed in MuSC transplants 1 day after transplantation (Figure S2E). Histological analyses 25 days after transplantation revealed a substantially larger contribution of fetal MuSCs to donor-derived, GFP[+] myofibers when compared to adult MuSCs (Figure 2E). BLI emission correlated with the number of GFP[+] myofibers in each individual transplant, confirming the extensive contribution of fetal MuSCs to muscle repair (Figure S2F).

preparations from both fetal and regenerating adult muscle contained both CD34[±] fractions (Figure S3D). Transplantation of 1,000 TdTomato^{+} MuSCs into *NOD/SCID* recipients confirmed the robust regenerative potential of fetal MuSC, albeit restricted to the CD34^{+} fraction, giving rise to a significantly higher number of donor myofibers than adult MuSCs (Figures 3A–3C). Activated adult MuSCs from regenerating muscle did not differ from freshly isolated adult MuSCs in their contribution to regenerating myofibers (Figures 3B and 3C), indicating that cell-cycle entry is not sufficient to alter behavior upon

Figure 2. Fetal MuSCs Robustly Contribute to Muscle Repair

(A) Scheme of fetal (E16.5) and adult (2 month) luciferase/EGFP MuSC transplantation, either 5,000 (3 days analyses) or 1,000 cells (25 days analyses) into the tibialis anterior muscles of NOD/SCID mice.

(B) Images of Pax7$^+$GFP$^+$ and Myod1$^+$GFP$^+$ donor cells 3 days post-transplantation. The scale bar represents 50 μm (left). Quantification of the percentage of Pax7$^+$ and Myod1$^+$ donor cells is shown (n = 5–6; right).

(C) Images of bioluminescence (BLI) emission in recipient mice at the indicated time points post-transplantation (photons s^{-1} cm^{-2}).

(D) Quantification of BLI emission following 1,000 or 10 MuSC transplantation over 25 days (n = 10–12).

(E) Images of GFP$^+$ donor myofibers 25 days post-transplantation. The scale bar represents 200 μm (left). Quantification of GFP$^+$ donor myofibers is shown (n = 10–12; right).

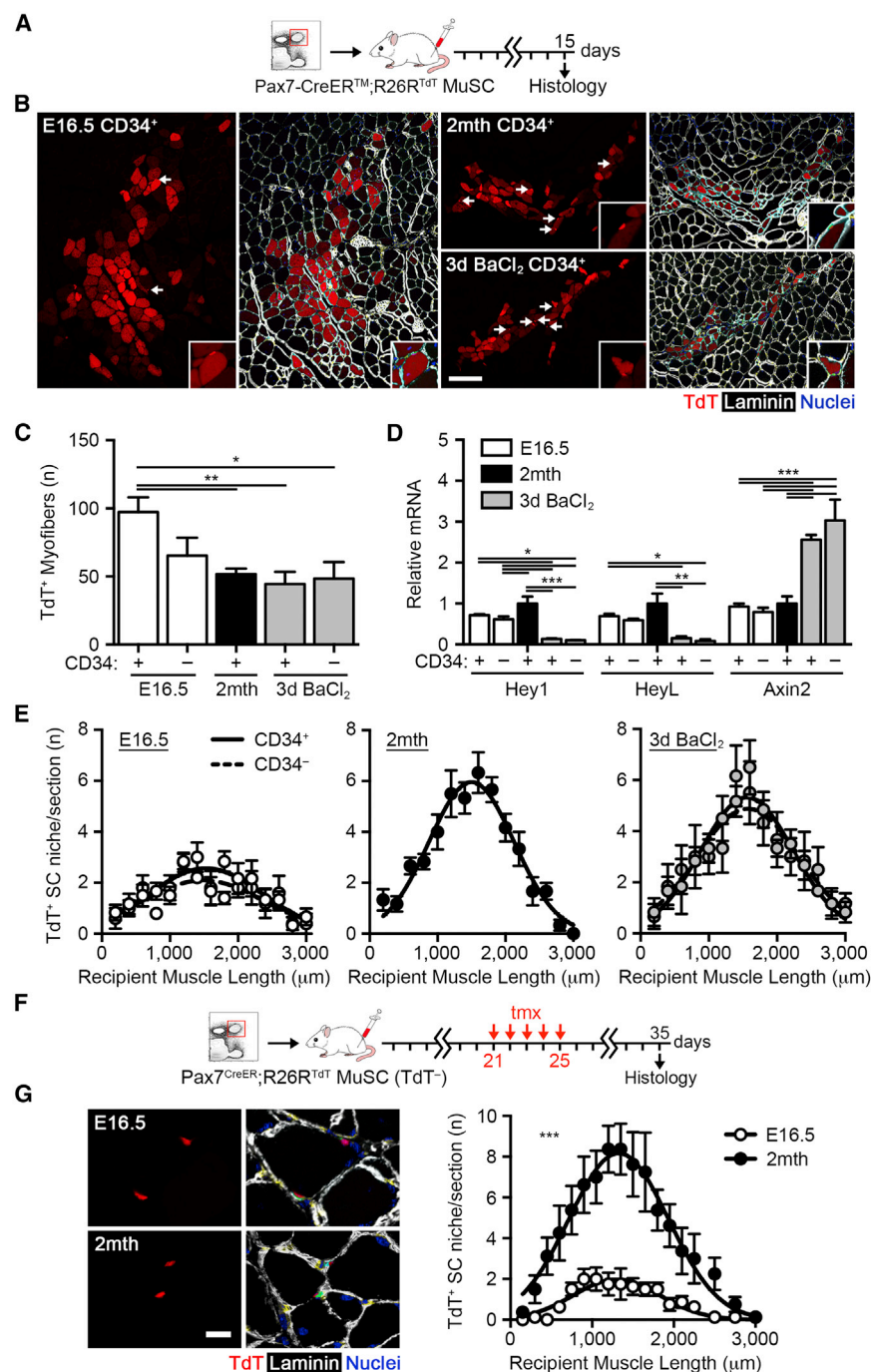Data are represented as average ± SEM (***p < 0.001, **p < 0.01, and *p < 0.05). See also Figure S2.

In addition, we investigated whether fetal MuSCs exhibited distinct signatures of signaling pathway activation. To this aim, we evaluated the activity of the Notch- and canonical Wnt-signaling pathways, both major regulators of MuSC function (Brack et al., 2008). Freshly isolated fetal MuSCs exhibited higher levels of Notch targets *Hey1* and *HeyL* and lower levels of the canonical Wnt target *Axin2* when compared to adult activated MuSCs (Figure 3D), a transcriptional signature associated with higher stemness. Taken together, these results demonstrate an inherent and robust expansion and regenerative potential of fetal MuSCs during tissue repair.

The Ability of MuSCs to Repopulate the Stem Cell Pool Increases during Development

MuSCs are purposed with two functions during skeletal muscle regeneration: to repair the damaged tissue and to replenish the stem cell pool for subsequent bouts of muscle repair (Shea et al., 2010). Taking advantage of the brightness of the TdTomato protein (Shaner et al., 2004), further assessment of primary transplantations performed with *Pax7-CreER^{TM};R26R^{TdT}* MuSCs revealed donor cell engraftment of both fetal and adult MuSCs into the adult satellite cell niche (Figure 3B). Intriguingly, we detected significantly fewer mononucleated, donor-derived fetal MuSCs underneath the basal lamina surrounding myofibers (Figures 3E and S3H). Neither fetal nor adult MuSCs were found interstitially. We speculate that this result likely reflects the responsibilities of fetal

transplantation. Donor myofiber cross-sectional area did not differ with fetal, adult, or activated adult transplantation (Figure S3E). To determine whether the presence of resident adult myofibers in recipient muscles may improve fetal MuSC fusion efficiency upon transplantation, we co-cultured EGFP$^+$ fetal MuSCs with TdTomato$^+$ adult MuSCs in differentiation conditions. Indeed, fetal and adult MuSCs were able to capably fuse together and the presence of adult MuSCs significantly improved the fusion efficiency of fetal MuSCs (Figures S3F and S3G).

Figure 3. The Ability of MuSCs to Repopulate the Stem Cell Pool Increases during Development

(A) Scheme of 1,000 Pax7-CreER™;R26R^{TdT} MuSC transplantation.

(B) Images of TdTomato$^+$ donor myofibers and satellite cells 15 days post-transplantation. The scale bar represents 50 μm. Arrows indicate TdTomato$^+$ donor cells engrafted into the satellite cell niche (inset).

(C) Quantification of the number of TdTomato$^+$ donor myofibers 15 days post-transplantation (n = 6).

(D) Hey1, HeyL, and Axin2 mRNA levels in freshly isolated Pax7-CreER™;R26R^{TdT} MuSCs (n = 3–5).

(E) Quantification of the number of TdTomato$^+$ donor cells engrafted into the satellite cell niche 15 days post-transplantation (n = 6).

(F) Scheme of TdTomato$^-$ Pax7-CreER™;R26R^{TdT} MuSC transplantation and tamoxifen (tmx) treatment from 21 to 25 days.

(G) Images of TdTomato$^+$ donor cells engrafted into the satellite cell niche 35 days post-transplantation. The scale bar represents 20 μm (left). Quantification of TdTomato$^+$ donor satellite cells is shown (n = 8; right).

Data are represented as average ± SEM (***p < 0.001, **p < 0.01, and *p < 0.05). See also Figure S3.

sults were obtained with this protocol, strengthening our finding that the proficiency of MuSCs for niche colonization increases during developmental myogenesis (Figure 3G).

Given the divergent behavior of fetal and adult MuSCs following transplantation, we examined the proliferative behavior and spatial localization of MuSCs throughout muscle development. EdU was administered for 24 hr prior to tissue harvest and subsequent histological assessment at fetal, neonatal (P7), juvenile (P21), and adult stages. The progressive entry of Pax7$^+$ cells into the satellite cell niche during development negatively correlated with EdU incorporation, associating niche colonization with cell-cycle exit during muscle development (Figure S3I). Therefore, the regenerative advantage of fetal MuSCs may come at the expense of stem cell pool re-population, suggesting a balance between either outcome that shifts postnatally during development.

The Distinct Functionality of Fetal MuSCs Is Lost over Rounds of Serial Transplantation

To more stringently assess the long-term self-renewal potential of fetal MuSCs, we performed serial transplantation assays (Hall et al., 2010; Rocheteau et al., 2012; Figure 4A). Fifteen
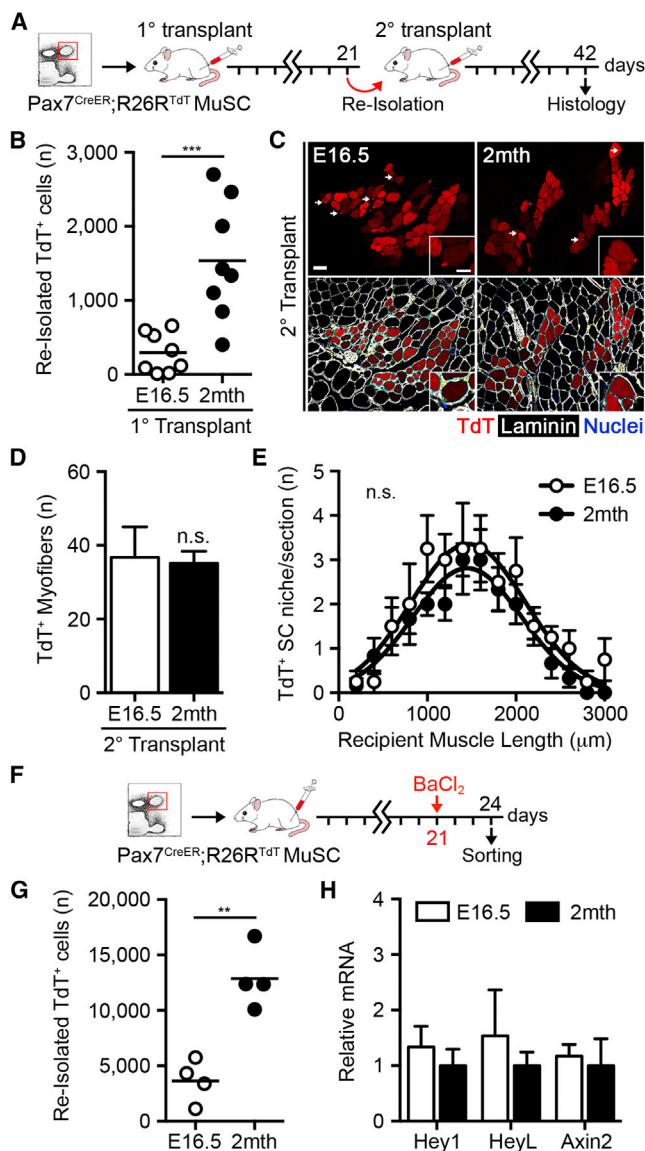
MuSCs in developing muscle, where the niche is not yet well formed and the majority contributes directly to muscle growth. We independently examined the ability of fetal MuSCs to occupy the satellite cell niche by transplanting 1,000 *Pax7-CreER^{TM};R26R^{TdT}* MuSCs sorted by FACS on the basis of α7-integrin and CD34 expression. Tmx was administered to recipient mice at 3 weeks post-transplantation, requiring that labeled cells express Pax7 following niche colonization (Figure 3F). Similar re-

Figure 4. The Distinct Functionality of Fetal MuSCs Is Lost over Rounds of Serial Transplantation
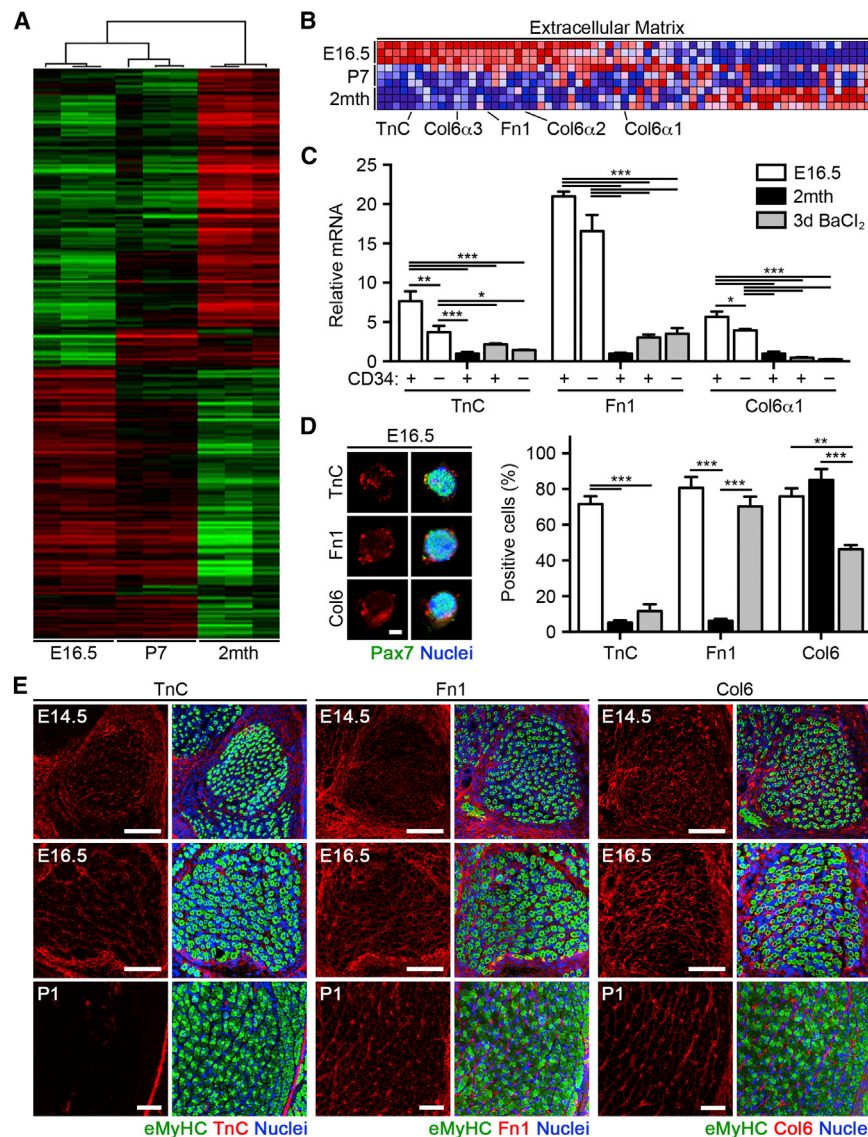
(A) Scheme of 15,000 $Pax7$-$CreER^{TM}$;$R26R^{TdT}$ MuSC serial transplantation.

(B) Quantification of TdTomato$^+$ cells re-isolated 21 days post-transplantation (n = 8).

(C) Images of TdTomato$^+$ donor myofibers 21 days post-secondary transplantation. The scale bar represents 50 μm.

(D) Quantification of TdTomato$^+$ donor myofibers 21 days post-secondary transplantation (n = 4–6).

(E) Quantification of TdTomato$^+$ donor cells engrafted into the satellite cell niche 21 days post-secondary transplantation (n = 4–6).

(F) Scheme of 15,000 $Pax7$-$CreER^{TM}$;$R26R^{TdT}$ MuSC transplantation, BaCl$_2$ injury at 21 days post-transplantation, and re-isolation 3 days post-injury.

(G) Quantification of TdTomato$^+$ MuSCs re-isolated 3 days post-injury (n = 4).

(H) $Hey1$, $HeyL$, and $Axin2$ mRNA levels in re-isolated TdTomato$^+$ MuSCs 3 days post-injury (n = 2–4).

Data are represented as average ± SEM (***p < 0.001 and **p < 0.01). See also Figure S4.

thousand $Pax7$-$CreER^{TM}$;$R26R^{TdT}$ MuSCs were transplanted into hind-limb-irradiated $NOD/SCID$ primary recipients and re-isolated by FACS 3 weeks post-transplantation. Consistent with prior results examining donor cell niche engraftment, significantly fewer TdTomato$^+$ fetal-derived cells were recovered from primary recipient muscles (Figures 4B and S4A). To evaluate the functional potential of serially transplanted fetal MuSCs, 500 re-isolated TdTomato$^+$ cells were transplanted into $NOD/SCID$ secondary recipient mice and harvested at 3 weeks for histological analysis. Fetal MuSCs were indeed able to contribute to a second round of regeneration, evidence of enduring self-renewal capacity (Figures 4C and 4D). Remarkably, serially transplanted fetal MuSCs no longer differed in their contribution to regenerating myofibers or the satellite cell niche, suggestive of behavioral adaptations over multiple rounds of regeneration (Figure 4E). To determine whether the activity of Notch and Wnt signaling is similarly changed in fetal MuSCs following engraftment, 15,000 $Pax7$-$CreER^{TM}$;$R26R^{TdT}$ MuSCs were transplanted into hind-limb-irradiated $NOD/SCID$ primary recipients. Recipient muscles were injured by BaCl$_2$ injection 21 days post-transplantation and re-isolated at 3 days post-injury to mimic the comparison made upon primary isolation (Figures 4F and S4B). Again, significantly fewer TdTomato$^+$ fetal-derived cells were recovered during re-isolation (Figure 4G). However, re-isolated fetal and adult MuSCs no longer differed in the expression of $Hey1$, $HeyL$, or $Axin2$ mRNA, consistent with their phenotypic adaptation following serial transplantation (Figure 4H). Collectively, these observations describe the distinct and intrinsically regulated functionality of fetal MuSCs with respect to both muscle repair and stem cell pool repopulation.

Fetal MuSCs Remodel Their Microenvironment via ECM Protein Secretion

We next asked what regulatory factors underlie the functional differences between MuSCs at various developmental stages. To this end, we performed comparative gene expression profiling in freshly isolated MuSCs from fetal (E16.5), early postnatal (P7), and adult (2 month) muscles. Microarray analyses identified ~1,700 differentially expressed genes between MuSCs after filtering (fold change > 2.0; p value < 0.01; Figures 5A and S5A). Gene clustering and principal-component analysis (PCA) demonstrated a gradual change in global gene expression, the fetal MuSCs transcriptome being more similar to neonatal rather than adult MuSCs (Figure S5B). Cellular development, growth, and proliferation and cell signaling were among the gene networks differentially regulated specifically in fetal MuSCs (Table S1). Gene set enrichment analysis (GSEA) demonstrated a significant upregulation of genes associated with the cell cycle and DNA replication in fetal MuSCs (Figure S5C; Table S2). On the other hand, MAPK, JAK/STAT, TGFβ, and Wnt signaling were enriched in adult MuSCs (Figure S5C), all pathways that display increased activity with adult MuSC activation and whose inhibition improves MuSC regenerative potential (Bernet et al., 2014; Brack et al., 2007, 2008; Carlson et al., 2008; Cosgrove et al., 2014; Palacios et al., 2010; Price et al., 2014; Tierney et al., 2014). Interestingly, several ECM genes were also enriched in fetal MuSCs (Figures 5B and S5D; Table S3). We hypothesized that autocrine ECM secretion might allow

Figure 5. Comparative Gene Expression Profiling of Fetal, Neonatal, and Adult MuSC

(A) Heatmap of differentially expressed genes in freshly isolated MuSCs by microarray analyses.

(B) Expression profiles for extracellular matrix (ECM) genes following gene set enrichment analysis (GSEA). Levels are indicated by shades of red (upregulation) and blue (downregulation).

(C) *TnC*, *Fn1*, and *Col6α1* mRNA levels in freshly isolated Pax7-CreER™;R26R^{TdT} MuSCs (n = 3–6).

(D) Images of MuSCs cultured in growth conditions for 2 hr. The scale bar represents 10 μm (left). Quantification of the percentage of TnC$^+$, Fn1$^+$, and Col6$^+$ cells is shown (n = 3; right).

(E) Images of TnC, Fn1, and Col6 expression in hind limb muscle at fetal and early postnatal stages. The scale bar represents 100 μm.

Data are represented as average ± SEM (***p < 0.001, **p < 0.01, and *p < 0.05). See also Figure S5 and Tables S1, S2, S3, and S4.

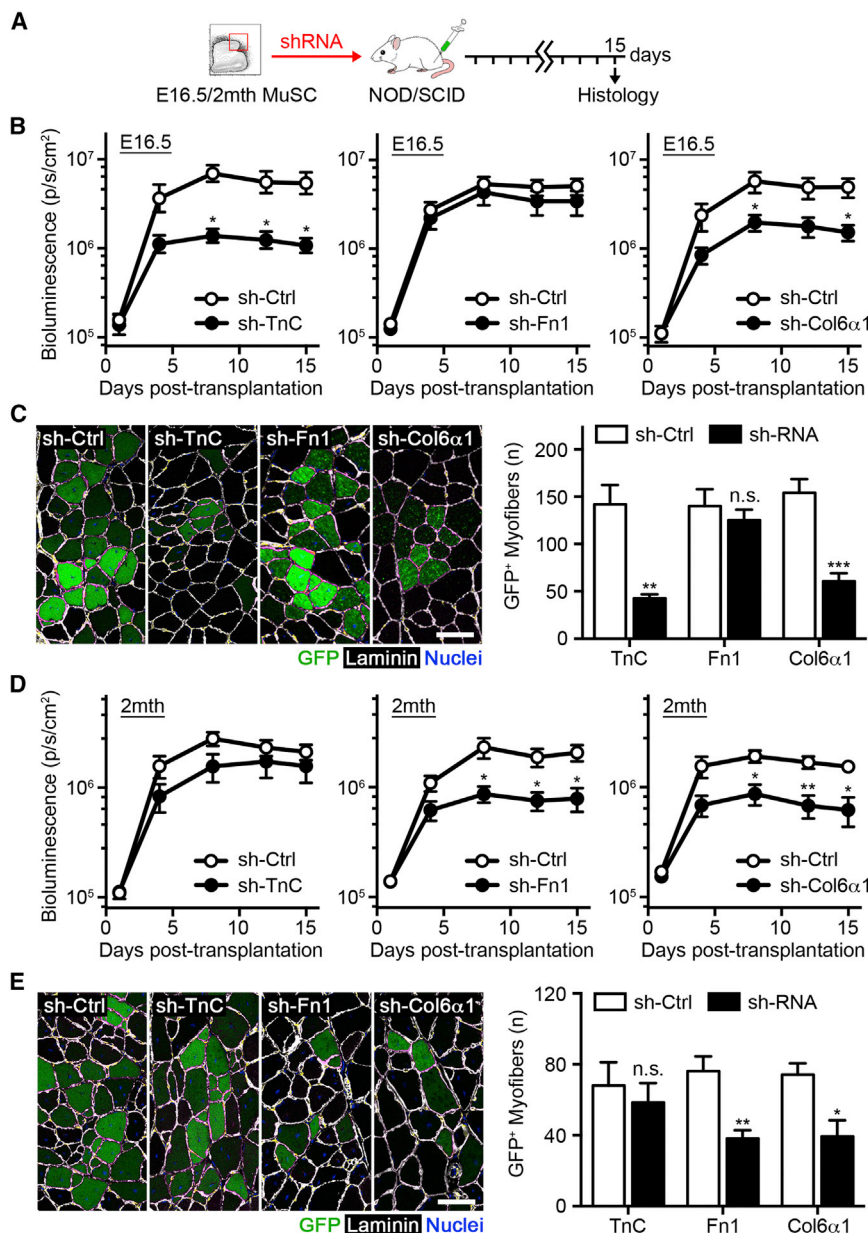Pax7$^+$ fetal MuSCs when compared to adult and activated adult MuSCs (Figures 5C and S5E). Given that all three subunits are required for intracellular assembly of functional collagen VI heterotrimers (Lamandé et al., 1998) and that *Col6α1* ablation is already known to reduce adult MuSC self-renewal capacity (Urciuolo et al., 2013), we chose to pursue Col6α1 in subsequent analyses. Immunostaining in freshly isolated Pax7$^+$ MuSCs demonstrated that a greater percentage of fetal MuSCs expressed TnC than both adult and activated adult MuSCs at the protein level (Figure 5D). A larger subset of fetal MuSCs expressed Fn1 when compared to adult MuSCs, but this difference was lost during adult MuSC activation. In contrast, collagen VI was expressed at equal levels in both fetal and adult MuSCs but significantly decreased in activated

fetal MuSCs to control their microenvironmental composition, thereby modulating cellular function to promote their expansion and contribution to muscle repair. Of these genes, tenascin-C (*TnC*) was among the most highly upregulated genes in fetal MuSCs as compared to adult MuSCs (Table S4). TnC influences multiple processes, including cell adhesion, inflammation, and communication between stem cells and other niche components (Chiquet-Ehrismann et al., 2014). Additionally, fibronectin (*Fn1*) and collagen VI alpha 3 (*Col6α3*) were highly expressed in fetal MuSC. Fibronectin and collagen VI have been previously shown to regulate adult MuSC behavior during muscle regeneration (Bentzinger et al., 2013; Urciuolo et al., 2013). Thus, we pursued TnC, Fn1, and collagen VI as potential candidates responsible for the enhanced contribution of fetal MuSCs to muscle repair.

We confirmed that *TnC*, *Fn1*, and the collagen VI subunits *Col6α1–3* were more highly expressed at the RNA level in

adult MuSCs, consistent with previous reports (Urciuolo et al., 2013). When cultured in growth conditions, all three ECM components maintained higher levels of expression in fetal rather than adult and activated adult MuSCs at the RNA level (Figure S5F). Interestingly, *TnC*, *Fn1*, and *Col6α1* transcript levels were downregulated in adult, but not fetal, MuSCs upon myogenic differentiation. However, immunostaining in differentiated MuSCs showed that TnC, Fn1, and collagen VI remained expressed only in undifferentiated cells and not in multinucleated myotubes (Figure S5G). All were abundantly present within the developing hind limb muscle bed at E14.5 and E16.5, surrounding eMyHC$^+$ myofibers (Figure 5E). TnC was largely absent from skeletal muscle 1 day after birth; it was only present in discrete, interstitial compartments and largely segregated to the epimysium and myotendinous junction. In contrast, Fn1 maintained its prenatal expression pattern through early postnatal stages whereas collagen VI remained into adulthood (Figure S5H).

Figure 6. Stage-Specific Role of ECM Proteins in Regulating MuSC Regenerative Potential

(A) Scheme of lentiviral *TnC*, *Fn1*, and *Col6α1* knockdown prior to 5,000 luciferase/EGFP MuSC transplantation.

(B) Quantification of BLI emission following fetal MuSC transplantation over 15 days, treated with sh-TnC, sh-Fn1, sh-Col6α1, or sh-control lentiviruses (n = 5).

(C) Images of fetal GFP$^+$ donor myofibers 15 days post-transplantation. The scale bar represents 100 μm (left). Quantification of GFP$^+$ donor myofibers is shown (n = 5; right).

(D) Quantification of BLI emission following adult MuSC transplantation over 15 days, treated with sh-TnC, sh-Fn1, sh-Col6α1, or sh-control lentiviruses (n = 5).

(E) Images of adult donor-derived GFP$^+$ myofibers 15 days post-transplantation. The scale bar represents 100 μm (left). Quantification of GFP$^+$ donor myofibers is shown (n = 5; right).

Data are represented as average ± SEM (**p < 0.01 and *p < 0.05). See also Figure S6.

MuSCs (Figure S6A). The effect of *TnC*, *Fn1*, and *Col6α1* knockdown during muscle repair was next examined by infecting freshly isolated fetal or adult MuSCs from luciferase x EGFP mice with either lentivirus or non-mammalian control overnight before transplantation into hind-limb-irradiated *NOD/SCID* mice (Figure 6A). *TnC* and *Col6α1* knockdown effectively impaired the ability of fetal MuSCs to expand in vivo, reducing engraftment levels by 76.5% ± 5.5% and 61.3% ± 8.7%, respectively, as assessed by BLI (Figures 6B and S6B). The contribution of donor-derived GFP$^+$ cells to muscle repair was also significantly diminished (Figure 6C). However, the loss of *Fn1* expression did not have any effect on fetal MuSC expansion or muscle repair (Figures 6B, 6C, and S6B), suggesting its demonstrated function in promoting MuSC self-renewal is specific to adulthood (Bentzinger et al., 2013).

Conversely, similar experiments examining the effect of *Fn1* and *Col6α1* knockdown in adult MuSCs confirmed their known role in promoting MuSC-mediated skeletal muscle repair (Bentzinger et al., 2013; Urciuolo et al., 2013), decreasing BLI engraftment levels, and reducing the number of donor-derived GFP$^+$ myofibers (Figures 6D, 6E, and S6B). On the other hand, *TnC* knockdown did not affect the ability of adult MuSCs to engraft and participate to tissue repair (Figures 6D, 6E, and S6B). This result likely reflects the already low levels of expression in adult MuSCs and identifies *TnC* as a fetal-specific regulator of MuSC regenerative potential. Whereas no effect on fetal MuSC survival was observed following *TnC* or *Fn1* downregulation, *Col6α1*
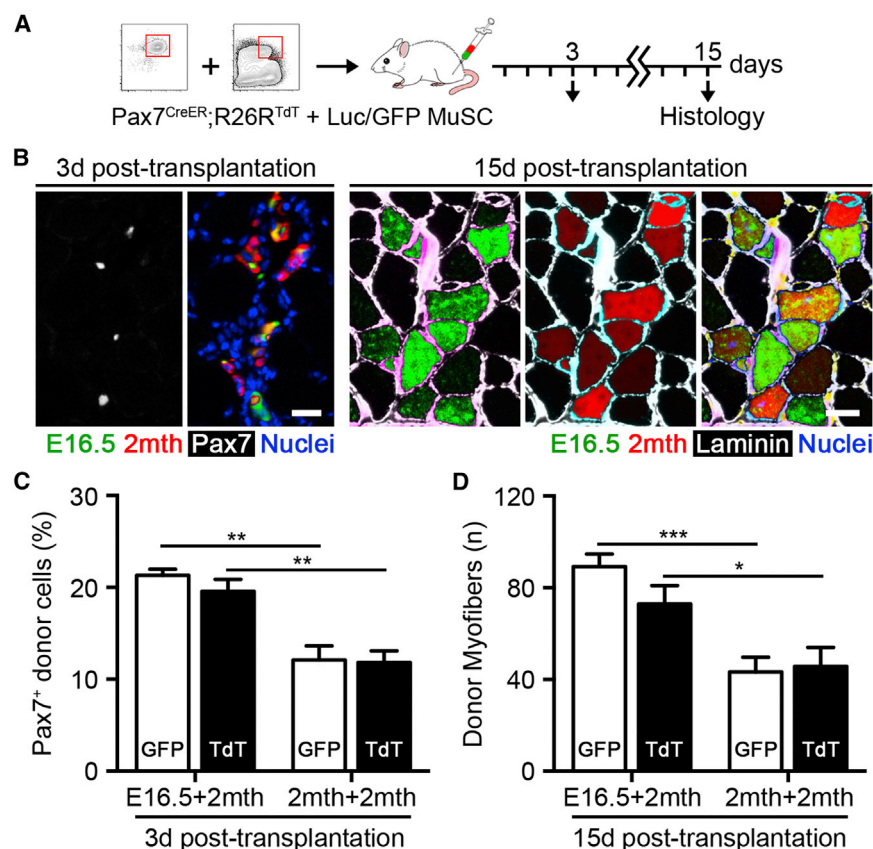
This transient deposition coupled with their differential expression in fetal MuSCs reinforces the notion that MuSCs remodel their own niche during developmental myogenesis. Together, these data implicate TnC, Fn1, and collagen VI each as dynamically regulated ECM proteins deposited during muscle development and suggest that they play a role in regulating the distinct functionality of fetal MuSCs.

ECM Proteins Play a Stage-Specific Role in Regulating MuSC Regenerative Potential

To investigate the functional role of MuSC-derived ECM protein expression, we performed loss-of-function studies in both fetal and adult MuSCs. Lentiviral shRNA infection efficiently downregulated *TnC*, *Fn1*, and *Col6α1* transcript levels in fetal and adult

Figure 7. Fetal MuSC Co-transplantation Enhances Adult MuSC Expansion and Muscle Repair

(A) Scheme of 1,000 fetal luciferase/EGFP and 1,000 adult Pax7-CreER™;R26R^{TdT} MuSCs co-transplantation.

(B) Images of Pax7$^+$GFP$^+$ and Pax7$^+$TdTomato$^+$ donor cells 3 days post-transplantation. The scale bar represents 20 μm (left). Images of GFP$^+$ and TdTomato$^+$ donor myofibers 15 days post-transplantation are shown. The scale bar represents 50 μm (right).

(C) Quantification of the percentage of Pax7$^+$ donor cells 3 days post-transplantation (n = 4).

(D) Quantification of GFP$^+$ and TdTomato$^+$ donor myofibers 15 days post-transplantation (n = 6).

Data are represented as average ± SEM (***p < 0.001, **p < 0.01, and *p < 0.05). See also Figure S7.

DISCUSSION

Here, we demonstrate that fetal MuSCs are capable of robust contribution to skeletal muscle repair and that this potential is progressively reduced after birth. Although MuSC-mediated regeneration in the adult often recapitulates developmental processes, tissue development and local repair are inherently different events that may require distinct stem cell functionality. MuSC activity during prenatal myogenesis is mainly purposed with their cellular contribution to myofibers, laying a foundation for subsequent muscle growth (White et al., 2010), and do not begin to enter the newly formed satellite cell niche until late fetal stages (Kassar-Duchossoy et al., 2005; Relaix et al., 2005). Conversely, adult MuSCs must both repair damaged muscle and ensure continued maintenance of the stem cell pool for future rounds of regeneration, actively repopulating the satellite cell niche. Our results support the notion that fetal MuSC behavior reflects their primary responsibilities within developing, rather than regenerating, muscle.

Paradoxically, fetal MuSCs more rapidly expand during the early stages of muscle repair but do not proportionally contribute to stem cell pool repopulation. Whereas we cannot rule out the possibility that fetal MuSCs proliferate as transient-amplifying muscle progenitors destined to terminally differentiate, increased Pax7 expression and Notch signaling but lower levels of canonical Wnt activity are characteristic of a stem cell state. We propose that niche entry, although often a suitable proxy for the predicted maintenance of self-renewal potential, is an indirect measure that is not a required characteristic of stem cells by definition and does not exclude the possibility of active self-renewal in cells that do not ultimately colonize the niche. The behavior of fetal MuSCs may represent a temporary uncoupling of satellite cell niche engraftment and self-renewal, associating enhanced tissue repair with sustained expansion of stem cell progeny whereas stem cell pool repopulation is partnered

knockdown did increase the percentage of TUNEL$^+$ cells, consistent with previous reports (Urciuolo et al., 2013). Taken together, these data provide evidence for the essential and stage-specific regulatory roles played by ECM proteins on MuSC function during muscle repair.

Fetal MuSC Co-transplantation Enhances Adult MuSC Expansion and Muscle Repair

Finally, we reasoned that fetal MuSC-derived secreted components might also promote adult MuSC function. To test this hypothesis, we performed co-transplantation experiments. TdTomato$^+$ adult MuSCs were obtained from *Pax7-CreER™; R26R^{TdT}* mice and co-transplanted with either fetal or adult MuSCs isolated from EGFP mice (Figure 7A). This experimental strategy was able to successfully present TnC, Fn1, and collagen VI to adult MuSCs at early time points during muscle repair (Figure S7). Accordingly, we observed a significant increase in the percentage of adult MuSCs expressing Pax7 at 3 days when co-transplanted with fetal MuSCs compared to adult control samples (Figures 7B and 7C). This coincided with significantly higher numbers of adult donor-derived myofibers 15 days post-transplantation (Figure 7D), improving the ability of adult MuSCs to both expand and contribute to muscle repair. These findings indicate that local microenvironmental remodeling by fetal MuSCs can act in a paracrine fashion to promote neighboring adult MuSC regenerative potential.

with re-entry into quiescence to preserve self-renewal potential. Furthermore, our study indicates that the autonomous secretion of TnC and collagen VI support fetal MuSC expansion whereas recent work has demonstrated that MuSCs at the same stage assemble distinct basal lamina components that promote niche colonization (Bröhl et al., 2012). It is tempting to speculate that distinct subpopulations of MuSC precursors modify their local microenvironments to accomplish either task, contributing to emerging stem cell heterogeneity during developmental myogenesis.

Our findings indicate that the fetal MuSC population adopts an adult-like phenotype upon serial transplantation, mimicking the functional transition that normally takes place during myogenic development. The regenerative event may select for those fetal MuSCs better able to repopulate the niche, leaving only these cells to be functionally assessed following re-isolation. Environmental factors may also guide their behavioral adaptation. Alterations in microenvironmental stimuli with niche occupancy leading to the induction of quiescence may act as a transformative process, imposing a modified functionality to participating fetal MuSCs.

In the present report, we show that fetal MuSCs modulate their microenvironment by the secretion of ECM proteins that are able to enhance stem cell function. ECM interactions are known to influence cell behavior through altered tissue stiffness and topography (Trappmann et al., 2012). Mechanistically, Fn1 has been shown to cooperate with Wnt7a to augment non-canonical Wnt signaling (Bentzinger et al., 2013), whereas collagen VI is responsible for modulating tissue stiffness and biomechanical properties (Urciuolo et al., 2013). Collagen VI has been shown to mediate proper Fn1 deposition and fibrillar arrangement, emphasizing the interconnected nature of ECM organization (Sabatelli et al., 2001). However, little is known about the possible function of TnC in skeletal muscle. TnC is a pleiotropic molecule, interacting with growth factors, ECM proteins, and membrane-bound receptors (Chiquet-Ehrismann et al., 1986; Midwood et al., 2009). Despite being apparently dispensable for normal development (Saga et al., 1992), TnC is present during organ morphogenesis and wound healing in multiple tissues and is a critical component of adult stem cell niches (Garcion et al., 2004; Nakamura-Ishizu et al., 2012). Both TnC and Fn1 have been shown to be key components of the transitional matrix following amphibian limb amputation by lowering tissue stiffness, promoting migration, and inhibiting terminal differentiation (Calve et al., 2010). Together with our study, these findings support a model in which ECM composition in the local microenvironment influences MuSC fate during muscle growth and repair.

Our co-transplantation results indicate that the overexpression of these ECM molecules might improve adult MuSC regenerative potential. Gain-of-function studies that impart adult stem cells with fetal characteristics have been shown to increase their long-term self-renewal potential (He et al., 2011). However, muscle degenerative pathologies often result in fibrotic scarring caused by dysregulated inflammatory cues and the persistence of matrix-producing cells, impairing muscle force production and regenerative potential (Brack et al., 2007; Lemos et al., 2015). Prospective therapies leveraging these ECM proteins for improving endogenous self-renewal potential may require only transient reactivation or more-specific, downstream targeting

to avoid these negative consequences. Alternatively, utilizing or engineering cells to favorably remodel their microenvironment over time may provide favorable biophysical cues able to promote muscle regeneration (Gilbert et al., 2010). This work would accelerate the development of tissue-engineering strategies aimed at de novo muscle formation and ameliorating the functional impairment of MuSCs in muscle-wasting conditions (Chakkalakal et al., 2012; Sousa-Victor et al., 2014).

In conclusion, our study has revealed that fetal MuSCs possess a remarkable regenerative potential through more-efficient expansion, intrinsically regulating their behavior through the selective expression of ECM proteins to remodel their local microenvironment. Future work will more comprehensively define the fetal niche composition and relevant cellular contributors working to promote either muscle formation or niche engraftment. This would potentially aid the identification of novel targets to direct stem cell activity toward the immediate or long-term aspects of tissue repair.

EXPERIMENTAL PROCEDURES

Animals

All animal protocols were approved by the Sanford Burnham Prebys Medical Discovery Institute (SBPMDI) Animal Care Committees. *Pax7CreER^TM* mice, a kind gift from C. Keller (Nishijo et al., 2009), were used to generate *Pax7-CreER^TM;R26R^TdT* mice. *Luciferase* mice were kindly provided by H. M. Blau (Stanford University). *EGFP* mice were kindly provided by B. Stallcup (SBPMDI). *C57BL/6*, *NOD/SCID*, and *R26R^TdT* mice were purchased from Jackson Laboratories.

MuSC Isolation

MuSCs were isolated as described previously with minor revisions (Sacco et al., 2008). See Supplemental Experimental Procedures for a detailed description of the procedure.

Cell Culture

Freshly isolated MuSCs were plated on tissue culture plates coated with laminin (Roche) and maintained in growth media (45% DMEM, 40% F10, 15% FBS, and 2.5 ng ml^{-1} basic fibroblast growth factor [bFGF]). Cell proliferation was measured by EdU incorporation (Life Technologies). For clonal analyses, MuSCs were plated individually by limiting dilution in 96-well plates and maintained in growth media for 5 days. Terminal myogenic differentiation was induced with DMEM and 2% horse serum for 3 days.

Lentiviral Infection

Lentiviruses were purchased from the MISSION shRNA library (Sigma) as part an agreement with the Sanford Consortium of Regenerative Medicine. Tissue culture plates were coated with laminin (20 μg ml^{-1}) for 45 min at 37°C, followed by retronectin (15 μg ml^{-1}) for 2 hr at room temperature. Plated MuSCs were infected with sh-TnC, sh-Fn1, sh-Col6α1, or non-mammalian control (sh-Ctrl) in growth media supplemented with 8 ng ml^{-1} polybrene (Sigma) overnight at 37°C and 5% CO$_2$.

Cell Transplantation and Tissue Injury

Prior to transplantation, *NOD/SCID* mice were anesthetized with an intraperitoneal (i.p.) injection of xylazine/ketamine solution and shielded in a lead jig to expose only the hind limbs to a single dose of 18 Gy radiation, administered within 1 day of cell transplantation. Freshly isolated MuSCs were resuspended in 15 μl PBS and injected intramuscularly into the TA muscles of recipient mice. For local tissue injury, mice were anesthetized with isoflurane and received a single 20-μl injection of barium chloride suspended in PBS (1.2% w/v; Sigma) into the TA muscles. To induce TdTomato expression in *Pax7-CreER^TM;R26R^TdT* mice or cells following engraftment, tmx resuspended in

corn oil was injected intraperitoneally (0.15 mg g^{-1} body weight; Sigma) for 5 days in adult mice or as a single injection in time-mated females.

BLI

A Xenogen-100 device was used as previously described (Sacco et al., 2008). After i.p. injection of luciferin suspended in PBS (0.1 mmol kg^{-1} body weight; Xenogen), images were acquired (60 s exposure; Living Image; Xenogen). See Supplemental Experimental Procedures for a detailed description of the procedure.

Immunofluorescence

Muscle tissues were prepared for histology as previously described (Sacco et al., 2005). Cells and muscle sections were fixed with 1.5% PFA, permeabilized in 0.1% Triton, and blocked in 20% goat serum. Incubation with the primary antibodies was performed overnight at 4°C. See Supplemental Experimental Procedures for a list of antibodies used. Cell death was measured by TUNEL assay (Roche). Images were acquired using an inverted epifluorescent microscope (Nikon TE300), CCD SPOT RT camera, and SPOT imaging software (Diagnostic Instruments) or a LSM170 laser-scanning confocal microscope, Plan-Apochromat 20×/0.8 or Plan NeoFluar 40×/1.3 oil objective lens, and ZEN 2011 imaging software (Zeiss). All images were composed and edited and modifications applied to the whole image using Photoshop CS6 (Adobe).

Microarray Analysis

Total RNA was extracted from freshly isolated MuSCs using a mirVana Kit (Ambion). Total RNA was quantified with the Qubit RNA HS Assay kit (Invitrogen), and RNA quality was assessed using a RNA6000 Nano kit (Agilent). One hundred nanograms RNA per sample was amplified using the Illumina Total Prep RNA Amplification kit (Ambion). 1,500 ng biotinylated RNA per sample was hybridized to Illumina MouseWG-6 v2.0 Expression BeadChips. All procedures were performed according to the manufacturer's protocol. Quality control was performed in GenomeStudio. Normalization was performed in R using the robust spline normalization (Du et al., 2008). Differential gene expression analysis was performed using GenePattern (Reich et al., 2006). Differentially expressed probes were selected for p value < 0.01 and fold change >2. Hierarchical gene clustering was performed in Cluster 3.0 followed by heatmap visualization using Java Treeview (Juan and Huang, 2007). PCA was performed using Qlucore Omics Explorer n.n (Qlucore AB). GSEA was performed comparing fetal and adult microarray datasets prior to filtering and differential expression analysis (Subramanian et al., 2005). Differentially expressed genes were analyzed for cellular component gene ontology (GO) with DAVID.

Statistical Analysis

Data are presented as mean ± SEM. Comparisons between groups used the Student's t test assuming two-tailed distributions with an alpha level of 0.05. Comparisons between three or more samples were performed using one- or two-way ANOVA with Tukey's HSD test. Clonal assays were analyzed by the Kruskal-Wallis non-parametric test with Dunn's post-test. Time-lapse assays were represented in contingency tables and analyzed by the chi-square test. Satellite cell niche engraftment data were fitted to a Gaussian distribution using least-squares (ordinary) method. All statistical tests were performed using GraphPad Prism 6 for Macintosh. All experiments requiring the use of animals were subjected to randomization based on litter. Investigators were not blinded to group allocation or outcome assessment. No samples or animals were excluded from this study.

ACCESSION NUMBERS

The accession number for the microarray analyses reported in this paper is GEO: GSE76989.

SUPPLEMENTAL INFORMATION

Supplemental Information includes Supplemental Experimental Procedures, seven figures, four tables, and two movies and can be found with this article online at http://dx.doi.org/10.1016/j.celrep.2016.01.072.

REFERENCES

Bentzinger, C.F., Wang, Y.X., and Rudnicki, M.A. (2012). Building muscle: molecular regulation of myogenesis. Cold Spring Harb. Perspect. Biol. *4*, a008342.

Bentzinger, C.F., Wang, Y.X., von Maltzahn, J., Soleimani, V.D., Yin, H., and Rudnicki, M.A. (2013). Fibronectin regulates Wnt7a signaling and satellite cell expansion. Cell Stem Cell *12*, 75–87.

Bernet, J.D., Doles, J.D., Hall, J.K., Kelly Tanaka, K., Carter, T.A., and Olwin, B.B. (2014). p38 MAPK signaling underlies a cell-autonomous loss of stem cell self-renewal in skeletal muscle of aged mice. Nat. Med. *20*, 265–271.

Biressi, S., Tagliafico, E., Lamorte, G., Monteverde, S., Tenedini, E., Roncaglia, E., Ferrari, S., Ferrari, S., Cusella-De Angelis, M.G., Tajbakhsh, S., and Cossu, G. (2007). Intrinsic phenotypic diversity of embryonic and fetal myoblasts is revealed by genome-wide gene expression analysis on purified cells. Dev. Biol. *304*, 633–651.

Brack, A.S., Conboy, M.J., Roy, S., Lee, M., Kuo, C.J., Keller, C., and Rando, T.A. (2007). Increased Wnt signaling during aging alters muscle stem cell fate and increases fibrosis. Science *317*, 807–810.

Brack, A.S., Conboy, I.M., Conboy, M.J., Shen, J., and Rando, T.A. (2008). A temporal switch from notch to Wnt signaling in muscle stem cells is necessary for normal adult myogenesis. Cell Stem Cell *2*, 50–59.

Bröhl, D., Vasyutina, E., Czajkowski, M.T., Griger, J., Rassek, C., Rahn, H.P., Purfürst, B., Wende, H., and Birchmeier, C. (2012). Colonization of the satellite cell niche by skeletal muscle progenitor cells depends on Notch signals. Dev. Cell *23*, 469–481.

Calve, S., Odelberg, S.J., and Simon, H.G. (2010). A transitional extracellular matrix instructs cell behavior during muscle regeneration. Dev. Biol. *344*, 259–271.

Carlson, M.E., Hsu, M., and Conboy, I.M. (2008). Imbalance between pSmad3 and Notch induces CDK inhibitors in old muscle stem cells. Nature *454*, 528–532.

Chakkalakal, J.V., Jones, K.M., Basson, M.A., and Brack, A.S. (2012). The aged niche disrupts muscle stem cell quiescence. Nature *490*, 355–360.

Chiquet-Ehrismann, R., Mackie, E.J., Pearson, C.A., and Sakakura, T. (1986). Tenascin: an extracellular matrix protein involved in tissue interactions during fetal development and oncogenesis. Cell *47*, 131–139.

Chiquet-Ehrismann, R., Orend, G., Chiquet, M., Tucker, R.P., and Midwood, K.S. (2014). Tenascins in stem cell niches. Matrix Biol. *37*, 112–123.

Collins, C.A., Olsen, I., Zammit, P.S., Heslop, L., Petrie, A., Partridge, T.A., and Morgan, J.E. (2005). Stem cell function, self-renewal, and behavioral heterogeneity of cells from the adult muscle satellite cell niche. Cell *122*, 289–301.

Cosgrove, B.D., Gilbert, P.M., Porpiglia, E., Mourkioti, F., Lee, S.P., Corbel, S.Y., Llewellyn, M.E., Delp, S.L., and Blau, H.M. (2014). Rejuvenation of the muscle stem cell population restores strength to injured aged muscles. Nat. Med. *20*, 255–264.

Davis, R.L., Weintraub, H., and Lassar, A.B. (1987). Expression of a single transfected cDNA converts fibroblasts to myoblasts. Cell *51*, 987–1000.

Du, P., Kibbe, W.A., and Lin, S.M. (2008). lumi: a pipeline for processing Illumina microarray. Bioinformatics *24*, 1547–1548.

Dumont, N.A., Wang, Y.X., and Rudnicki, M.A. (2015). Intrinsic and extrinsic mechanisms regulating satellite cell function. Development *142*, 1572–1581.

Garcion, E., Halilagic, A., Faissner, A., and ffrench-Constant, C. (2004). Generation of an environmental niche for neural stem cell development by the extracellular matrix molecule tenascin C. Development *131*, 3423–3432.

Gilbert, P.M., Havenstrite, K.L., Magnusson, K.E., Sacco, A., Leonardi, N.A., Kraft, P., Nguyen, N.K., Thrun, S., Lutolf, M.P., and Blau, H.M. (2010). Substrate elasticity regulates skeletal muscle stem cell self-renewal in culture. Science *329*, 1078–1081.

Gros, J., Manceau, M., Thomé, V., and Marcelle, C. (2005). A common somitic origin for embryonic muscle progenitors and satellite cells. Nature *435*, 954–958.

Hall, J.K., Banks, G.B., Chamberlain, J.S., and Olwin, B.B. (2010). Prevention of muscle aging by myofiber-associated satellite cell transplantation. Sci. Transl. Med. *2*, 57ra83.

He, S., Kim, I., Lim, M.S., and Morrison, S.J. (2011). Sox17 expression confers self-renewal potential and fetal stem cell characteristics upon adult hematopoietic progenitors. Genes Dev. *25*, 1613–1627.

Heslop, L., Morgan, J.E., and Partridge, T.A. (2000). Evidence for a myogenic stem cell that is exhausted in dystrophic muscle. J. Cell Sci. *113*, 2299–2308.

Hutcheson, D.A., Zhao, J., Merrell, A., Haldar, M., and Kardon, G. (2009). Embryonic and fetal limb myogenic cells are derived from developmentally distinct progenitors and have different requirements for beta-catenin. Genes Dev. *23*, 997–1013.

Juan, H.F., and Huang, H.C. (2007). Bioinformatics: microarray data clustering and functional classification. Methods Mol. Biol. *382*, 405–416.

Kassar-Duchossoy, L., Giacone, E., Gayraud-Morel, B., Jory, A., Gomès, D., and Tajbakhsh, S. (2005). Pax3/Pax7 mark a novel population of primitive myogenic cells during development. Genes Dev. *19*, 1426–1431.

L'honoré, A., Commère, P.H., Ouimette, J.F., Montarras, D., Drouin, J., and Buckingham, M. (2014). Redox regulation by Pitx2 and Pitx3 is critical for fetal myogenesis. Dev. Cell *29*, 392–405.

Lamandé, S.R., Sigalas, E., Pan, T.C., Chu, M.L., Dziadek, M., Timpl, R., and Bateman, J.F. (1998). The role of the alpha3(VI) chain in collagen VI assembly. Expression of an alpha3(VI) chain lacking N-terminal modules N10-N7 restores collagen VI assembly, secretion, and matrix deposition in an alpha3(VI)-deficient cell line. J. Biol. Chem. *273*, 7423–7430.

Lemos, D.R., Babaeijandaghi, F., Low, M., Chang, C.K., Lee, S.T., Fiore, D., Zhang, R.H., Natarajan, A., Nedospasov, S.A., and Rossi, F.M. (2015). Nilotinib reduces muscle fibrosis in chronic muscle injury by promoting TNF-mediated apoptosis of fibro/adipogenic progenitors. Nat. Med. *21*, 786–794.

Lepper, C., Partridge, T.A., and Fan, C.M. (2011). An absolute requirement for Pax7-positive satellite cells in acute injury-induced skeletal muscle regeneration. Development *138*, 3639–3646.

Madisen, L., Zwingman, T.A., Sunkin, S.M., Oh, S.W., Zariwala, H.A., Gu, H., Ng, L.L., Palmiter, R.D., Hawrylycz, M.J., Jones, A.R., et al. (2010). A robust and high-throughput Cre reporting and characterization system for the whole mouse brain. Nat. Neurosci. *13*, 133–140.

Messina, G., Biressi, S., Monteverde, S., Magli, A., Cassano, M., Perani, L., Roncaglia, E., Tagliafico, E., Starnes, L., Campbell, C.E., et al. (2010). Nfix regulates fetal-specific transcription in developing skeletal muscle. Cell *140*, 554–566.

Midwood, K., Sacre, S., Piccinini, A.M., Inglis, J., Trebaul, A., Chan, E., Drexler, S., Sofat, N., Kashiwagi, M., Orend, G., et al. (2009). Tenascin-C is an endogenous activator of Toll-like receptor 4 that is essential for maintaining inflammation in arthritic joint disease. Nat. Med. *15*, 774–780.

Montarras, D., Morgan, J., Collins, C., Relaix, F., Zaffran, S., Cumano, A., Partridge, T., and Buckingham, M. (2005). Direct isolation of satellite cells for skeletal muscle regeneration. Science *309*, 2064–2067.

Nakamura-Ishizu, A., Okuno, Y., Omatsu, Y., Okabe, K., Morimoto, J., Uede, T., Nagasawa, T., Suda, T., and Kubota, Y. (2012). Extracellular matrix protein tenascin-C is required in the bone marrow microenvironment primed for hematopoietic regeneration. Blood *119*, 5429–5437.

Nishijo, K., Hosoyama, T., Bjornson, C.R., Schaffer, B.S., Prajapati, S.I., Bahadur, A.N., Hansen, M.S., Blandford, M.C., McCleish, A.T., Rubin, B.P., et al. (2009). Biomarker system for studying muscle, stem cells, and cancer in vivo. FASEB J. *23*, 2681–2690.

Palacios, D., Mozzetta, C., Consalvi, S., Caretti, G., Saccone, V., Proserpio, V., Marquez, V.E., Valente, S., Mai, A., Forcales, S.V., et al. (2010). TNF/p38α/polycomb signaling to Pax7 locus in satellite cells links inflammation to the epigenetic control of muscle regeneration. Cell Stem Cell *7*, 455–469.

Price, F.D., von Maltzahn, J., Bentzinger, C.F., Dumont, N.A., Yin, H., Chang, N.C., Wilson, D.H., Frenette, J., and Rudnicki, M.A. (2014). Inhibition of JAK-STAT signaling stimulates adult satellite cell function. Nat. Med. *20*, 1174–1181.

Reich, M., Liefeld, T., Gould, J., Lerner, J., Tamayo, P., and Mesirov, J.P. (2006). GenePattern 2.0. Nat. Genet. *38*, 500–501.

Relaix, F., Rocancourt, D., Mansouri, A., and Buckingham, M. (2005). A Pax3/Pax7-dependent population of skeletal muscle progenitor cells. Nature *435*, 948–953.

Relaix, F., Montarras, D., Zaffran, S., Gayraud-Morel, B., Rocancourt, D., Tajbakhsh, S., Mansouri, A., Cumano, A., and Buckingham, M. (2006). Pax3 and Pax7 have distinct and overlapping functions in adult muscle progenitor cells. J. Cell Biol. *172*, 91–102.

Rocheteau, P., Gayraud-Morel, B., Siegl-Cachedenier, I., Blasco, M.A., and Tajbakhsh, S. (2012). A subpopulation of adult skeletal muscle stem cells retains all template DNA strands after cell division. Cell *148*, 112–125.

Sabatelli, P., Bonaldo, P., Lattanzi, G., Braghetta, P., Bergamin, N., Capanni, C., Mattioli, E., Columbaro, M., Ognibene, A., Pepe, G., et al. (2001). Collagen VI deficiency affects the organization of fibronectin in the extracellular matrix of cultured fibroblasts. Matrix Biol. *20*, 475–486.

Sacco, A., Doyonnas, R., LaBarge, M.A., Hammer, M.M., Kraft, P., and Blau, H.M. (2005). IGF-I increases bone marrow contribution to adult skeletal muscle and enhances the fusion of myelomonocytic precursors. J. Cell Biol. *171*, 483–492.

Sacco, A., Doyonnas, R., Kraft, P., Vitorovic, S., and Blau, H.M. (2008). Self-renewal and expansion of single transplanted muscle stem cells. Nature *456*, 502–506.

Sacco, A., Mourkioti, F., Tran, R., Choi, J., Llewellyn, M., Kraft, P., Shkreli, M., Delp, S., Pomerantz, J.H., Artandi, S.E., and Blau, H.M. (2010). Short telomeres and stem cell exhaustion model Duchenne muscular dystrophy in mdx/mTR mice. Cell *143*, 1059–1071.

Saga, Y., Yagi, T., Ikawa, Y., Sakakura, T., and Aizawa, S. (1992). Mice develop normally without tenascin. Genes Dev. *6*, 1821–1831.

Sambasivan, R., Yao, R., Kissenpfennig, A., Van Wittenberghe, L., Paldi, A., Gayraud-Morel, B., Guenou, H., Malissen, B., Tajbakhsh, S., and Galy, A. (2011). Pax7-expressing satellite cells are indispensable for adult skeletal muscle regeneration. Development *138*, 3647–3656.

Seale, P., Sabourin, L.A., Girgis-Gabardo, A., Mansouri, A., Gruss, P., and Rudnicki, M.A. (2000). Pax7 is required for the specification of myogenic satellite cells. Cell *102*, 777–786.

Shaner, N.C., Campbell, R.E., Steinbach, P.A., Giepmans, B.N., Palmer, A.E., and Tsien, R.Y. (2004). Improved monomeric red, orange and yellow fluorescent proteins derived from Discosoma sp. red fluorescent protein. Nat. Biotechnol. *22*, 1567–1572.

Shea, K.L., Xiang, W., LaPorta, V.S., Licht, J.D., Keller, C., Basson, M.A., and Brack, A.S. (2010). Sprouty1 regulates reversible quiescence of a self-renewing adult muscle stem cell pool during regeneration. Cell Stem Cell *6*, 117–129.

Sousa-Victor, P., Gutarra, S., García-Prat, L., Rodriguez-Ubreva, J., Ortet, L., Ruiz-Bonilla, V., Jardí, M., Ballestar, E., González, S., Serrano, A.L., et al. (2014). Geriatric muscle stem cells switch reversible quiescence into senescence. Nature *506*, 316–321.

Subramanian, A., Tamayo, P., Mootha, V.K., Mukherjee, S., Ebert, B.L., Gillette, M.A., Paulovich, A., Pomeroy, S.L., Golub, T.R., Lander, E.S., and Mesirov, J.P. (2005). Gene set enrichment analysis: a knowledge-based approach for interpreting genome-wide expression profiles. Proc. Natl. Acad. Sci. USA *102*, 15545–15550.

Tierney, M.T., Aydogdu, T., Sala, D., Malecova, B., Gatto, S., Puri, P.L., Latella, L., and Sacco, A. (2014). STAT3 signaling controls satellite cell expansion and skeletal muscle repair. Nat. Med. *20*, 1182–1186.

Trappmann, B., Gautrot, J.E., Connelly, J.T., Strange, D.G., Li, Y., Oyen, M.L., Cohen Stuart, M.A., Boehm, H., Li, B., Vogel, V., et al. (2012). Extracellular-matrix tethering regulates stem-cell fate. Nat. Mater. *11*, 642–649.

Urciuolo, A., Quarta, M., Morbidoni, V., Gattazzo, F., Molon, S., Grumati, P., Montemurro, F., Tedesco, F.S., Blaauw, B., Cossu, G., et al. (2013). Collagen VI regulates satellite cell self-renewal and muscle regeneration. Nat. Commun. *4*, 1964.

White, R.B., Biérinx, A.S., Gnocchi, V.F., and Zammit, P.S. (2010). Dynamics of muscle fibre growth during postnatal mouse development. BMC Dev. Biol. *10*, 21.

Zammit, P.S., Golding, J.P., Nagata, Y., Hudon, V., Partridge, T.A., and Beauchamp, J.R. (2004). Muscle satellite cells adopt divergent fates: a mechanism for self-renewal? J. Cell Biol. *166*, 347–357.